Flexible Transparent Films Based on Nanocomposite Networks of Polyaniline and Carbon Nanotubes for High-Performance Gas Sensing

Pengbo Wan, Xuemei Wen, Chaozheng Sun, Bevita K. Chandran, Han Zhang, Xiaoming Sun,* and Xiaodong Chen**

***A** flexible, transparent, chemical gas sensor is assembled from a transparent conducting film of carbon nanotube (CNT) networks that are coated with hierarchically nanostructured polyaniline (PANI) nanorods. The nanocomposite film is synthesized by in-situ, chemical oxidative polymerization of aniline in a functional multiwalled CNT (FMWCNT) suspension and is simultaneously deposited onto a flexible polyethylene terephthalate (PET) substrate. An as-prepared flexible transparent chemical gas sensor exhibits excellent transparency of 85.0% at 550 nm using the PANI/FMWCNT nanocomposite film prepared over a reaction time of 8 h. The sensor also shows good flexibility, without any obvious decrease in performance after 500 bending/extending cycles, demonstrating high-performance, portable gas sensing at room temperature. This superior performance could be attributed to the improved electron transport and collection due to the CNTs, resulting in reliable and efficient sensing, as well as the high surface-to-volume ratio of the hierarchically nanostructured composites. The excellent transparency, improved sensing performance, and superior flexibility of the device, may enable the integration of this simple, low-cost, gas sensor into handheld flexible transparent electronic circuitry and optoelectronic devices.*

1. Introduction

Flexible and transparent conductive films have gained immense popularity in recent years as these have applications in a wide variety of fields, such as communication, healthcare monitoring, and energy storage.[1–17] Their numerous applications are related to their portability and compatibility with plastic substrates, in addition to their inherent flexibility and transparency. These properties have been advantageously utilized in touch screens, supercapacitors, lithium-ion batteries and solar cells, to give a few examples.[18–23] Herein, we have attempted to endow these attributes to gas detectors. Flexible-transparent gas sensors are envisioned to be crucial components in portable electronic devices, which could provide ultra-sensitive and highly selective real-time analysis for healthcare and environmental monitoring. However, traditional gas detectors, which are mostly made from solid powder-like gas-sensing materials deposited on ceramic tubes or inter-finger probes,[24,25] do not possess the required flexibility or transparency. Hence, there exists a need to develop high-performance gas sensors that are based on transparent and flexible materials.

Various one-dimensional or quasi-one-dimensional nanomaterials have been investigated for use in flexible and transparent electronic devices. Among these, carbon-nanotube (CNT) network based films are prevalent due to their

Dr. P. B. Wan, X. M. Wen, C. Z. Sun, Prof. X. M. Sun
State Key Laboratory of Chemical Resource Engineering
Beijing University of Chemical Technology
P.O. Box 98, Beijing 100029, P.R. China
E-mail: pbwan@mail.buct.edu.cn;
sunxm@mail.buct.edu.cn

B. K. Chandran, Prof. X. Chen
School of Materials Science and Engineering
Nanyang Technological University
50 Nanyang Avenue, Singapore 639798, Singapore
E-mail: chenxd@ntu.edu.sg

Prof. H. Zhang
SZU-NUS Collaborative Innovation Centre
for Optoelectronic Science & Technology
and College of Optoelectronic Engineering
Shenzhen University
Shenzhen 518060, P.R. China

DOI: 10.1002/smll.201501772

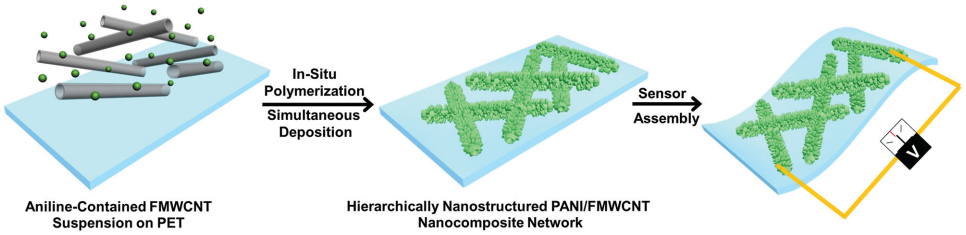

Scheme 1. Schematic illustration of the preparation of the hierarchically nanostructured PANI/FMWCNT nanocomposite network film by in situ chemical oxidative polymerization of aniline in CNT suspension with the assistance of CNT templates, with simultaneous deposition on a flexible PET substrate, and the fabrication of a flexible transparent chemical gas sensor using silver paint for circuit connection.

excellent optical transparency, electrical conductivity, intrinsic mobility, chemical stability, high surface area, and good flexibility.[15,26–33] However, the chemical gas-sensing performance of sensor devices based on CNT network films with high electrical conductivities (a sheet resistance of around 100 Ω/□ at a transmittance of ca. 80%),[34] has been unsatisfactory so far.[29] CNT films have been employed to recognize gaseous analytes, but these demonstrated a relatively low sensing performance and no transparency.[35] Therefore, the possibility of incorporating the needed transparency, flexibility, and high sensing performance into gas detectors that are based purely on a CNT network film remains limited.

Conducting polymers, such as those used in organic electronic devices, have many favorable properties, such as a low-temperature synthesis process, inherent compatibility with plastic substrates, and scalable and low-cost manufacturing, which make them suitable for wearable gas-sensing devices.[36–41] However, the limited optical transparency and environmental instability of nanostructured conducting polymer films are major drawbacks of these compounds. For example, polyaniline (PANI) network films have thus far not been able to replace indium tin oxide (ITO) in transparent electronics because their transparency of 65% is not adequate enough. Recently though, nanocomposites of PANI and CNTs prepared using CNT templates have demonstrated efficient charge transport and charge collection, and enhanced chemical and thermal stabilities. As such they were employed as the electrode material of energy-storage devices and sensing devices to detect pH values and vapor analytes.[42–45] Hence, it may be useful to explore whether this combination will provide synergistic advantages for gas sensors as well. By incorporating conducting polymers with a lower electrical conductivity into a highly conductive CNT network, a decreased conductivity of the nanocomposite may be obtained. However, in contrast to CNT films, at the same time a good transparency and chemical stability may be maintained, thus decoupling the transparency and the sensing performance in this type of gas detector. Furthermore, this combination can result in a relatively high carrier mobility, high surface-to-volume ratios, and short and direct paths for charge/ion transportation.

Herein, a nanocomposite film was synthesized by in-situ, chemical oxidative polymerization of aniline in a functional multiwalled CNT (FMWCNT) suspension that was simultaneously deposited onto a flexible polyethylene terephthalate (PET) substrate. The as-prepared PANI/FMWCNT nanocomposite network film was assembled into a gas-sensor device. The sensor exhibited a transparency of 85.0% at 550 nm for a PANI/FMWCNT nanocomposite film prepared using a reaction time of 8 h. Moreover, the device demonstrated excellent sensitivity at room temperature without any obvious decrease in performance after 500 bending/extending cycles (**Scheme 1**).

2. Results and Discussion

Essentially, the PANI nanorods were grown on the surface of FMWCNTs that are concurrently being deposited on a PET substrate, under different polymerization time periods, to form PANI/FMWCNT nanocomposite network films. Various oxygenated functional groups (e.g., carbonyl, hydroxyl, and epoxy groups) and benzene sulfonate were introduced into the FMWCNTs (**Figure 1**), after treatment with inorganic acid and coating with sodium dodecyl benzene sulfonate (SDBS), see Experimental Section for details. This provides good dispersibility and solubility of the CNTs in aqueous solutions, and directs the arrangement of anilinium ions around the tubes through electrostatic interaction for further polymerization of PANI.[44–47] The PET substrates were dipped into the FMWCNT suspension with an aniline concentration of 0.01 M and a ratio of [aniline]/[ammonium persulfate (APS)] of 1.75:1. The polymerization of aniline was carried out for different time spans, to obtain nanostructured nanocomposites networks with variable transparency and conductivity. During this process, the oxygenated functional groups likely act as active sites for attaching of the polymerized PANI onto the surface of the FMWCNTs. **Figure 2**a-d depicts the random nanocomposite networks formed at reaction times of 6 h, 8 h, 10 h, and 12 h, respectively. The nanostructured composites, having tiny protuberances on the surface of the FMWCNTs, were observed to form particle-like aggregates and few interconnected network structures

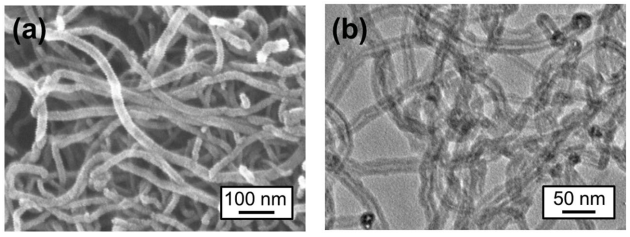

Figure 1. a) Scanning Electron Microscope (SEM) image and b) Transmission Electron Microscope (TEM) image of FMWCNTs.

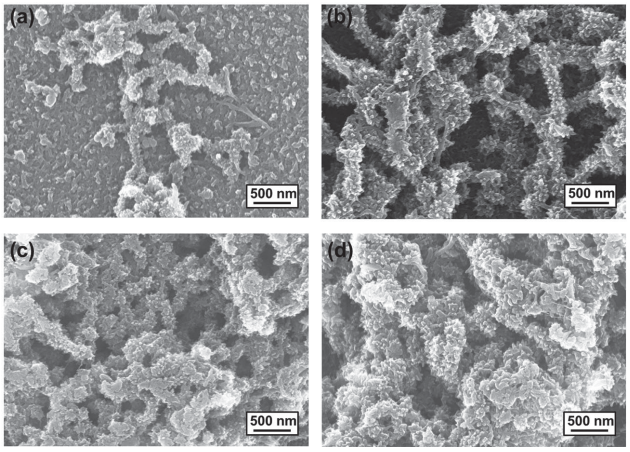

Figure 2. SEM images of hierarchically nanostructured PANI/FMWCNT nanocomposite networks after polymerization at a) 6 h, b) 8 h, c) 10 h, and d) 12 h.

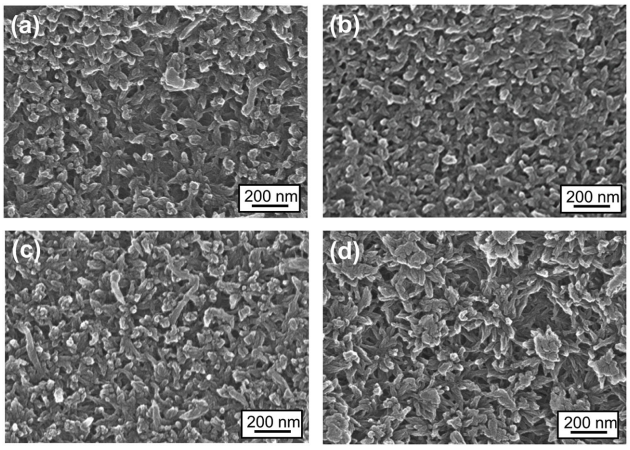

Figure 4. SEM image of pure PANI polymerized on the surface of the PET substrate after a polymerization time of a) 6 h, b) 8 h, c) 10 h, and d) 12 h.

at a reaction time of 6 h (Figure 2a). The presence of protuberances may be related to the large amount of active sites on the FMWCNT surface. The functional groups can attach to the anilinium ions via electrostatic attraction and serve as active sites for polymerization in the presence of APS, which could then act as the "seeds" for the following polymerization. In the successive polymerizations, hierarchical nanocomposites of the PANI nanorods grew on the surface of the FMWCNTs leading to an increase in number and size of the protuberances (Figure 2b, **Figure 3**, and Figure S2, Supporting Information).

When the polymerization was allowed to continue, excessive nanocomposites were formed, which covered the original random network structure to form dense nanocomposite films (Figure 2c,d). For comparison, PET films were dipped into the same aniline polymerizing solution in the absence of the suspension of FMWCNTs for the same time periods as before. In this case, particle-like PANI aggregates were obtained, as shown in **Figure 4**, implying that the FMWCNTs act as templates for the fabrication of the nanocomposite network. Moreover, the conductivity and transparency of the PANI/FMWCNT nanocomposite network films varied depending on the polymerization time. The sheet resistances of the PANI/FMWCNT nanocomposite network films polymerized for 6 h, 8 h, 10 h, and 12 h were 262 kΩ/□, 425 kΩ/□, 600 kΩ/□, 454 kΩ/□, respectively. At the same time, the transparency of these films at 550 nm showed a small variation from 84.2% to 85.0%, 85.9%, and 83.5% for the films polymerized for 6 h, 8 h, 10 h and 12 h, respectively, as demonstrated in **Figure 5**a. Notably, the nanostructured composite network films all showed excellent transparency over the wavelength range of 400 to 800 nm with a maximum transmittance of 85.5% (Figure 5a, 8 h sample). In comparison, films based on particle-like PANI aggregates prepared in the absence of CNT templates were less transparent than the nanostructured composite network films prepared for the same polymerization time (Figure S3, Supporting Information). For example, the transparency for the nanostructured composite network film after 8 h polymerization is 85.0% at 550 nm, compared to around 75.5% for the film based on particle-like PANI aggregates after 8 h polymerization, indi-

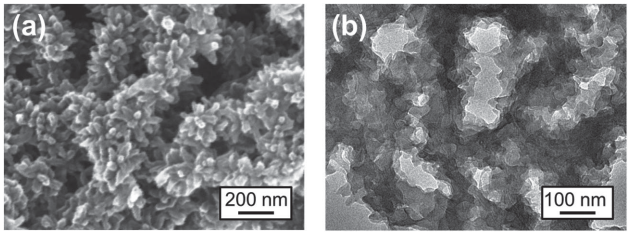

Figure 3. a) SEM image and b) TEM image of PANI/FMWCNT nanocomposite networks after a polymerization time of 8 h.

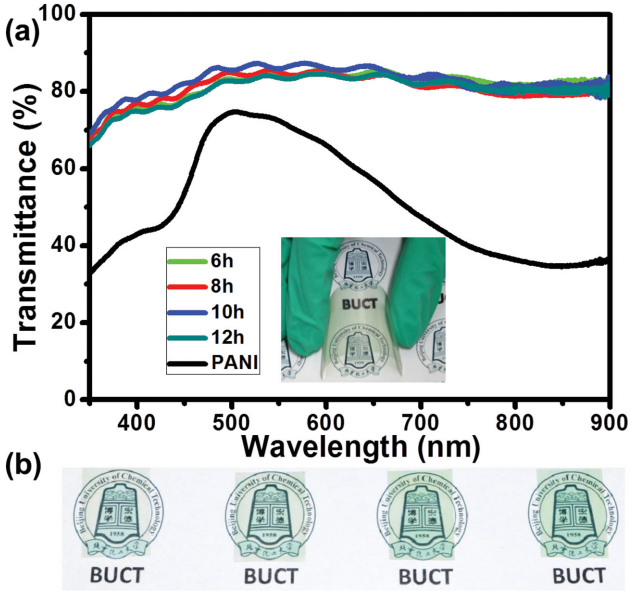

Figure 5. a) Transmittance spectra of the PANI/FMWCNT nanocomposite network films polymerized for 6 h, 8 h, 10 h and 12 h, and the particle-like PANI aggregate film prepared with a reaction time of 8 h. Inset: the flexible transparent PANI/FMWCNT nanocomposite network film. b) Photographs of the PANI/FMWCNT nanocomposite network films prepared using a reaction time of 6 h, 8 h, 10 h, and 12 h (from left to right). The school badge was placed behind the films.

www.MaterialsViews.com

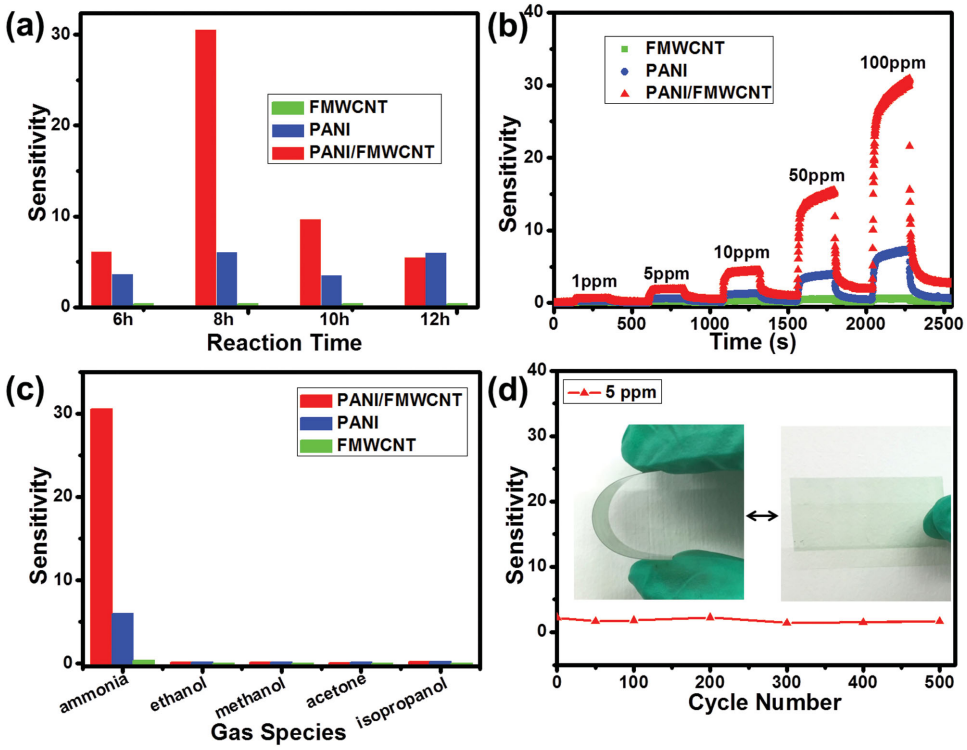

Figure 6. a) Gas-sensing sensitivity of the PANI/FMWCNT nanocomposite network, the particle-like PANI aggregate, and the FMWCNT film devices fabricated at different polymerization times, upon exposure to 100 ppm NH_3 at room temperature. b) Gas-sensing performance of the PANI/FMWCNT nanocomposite, the particle-like PANI aggregate, and the FMWCNT film devices fabricated at a polymerization time of 8 h to different concentrations of NH_3 ranging from 1 ppm to 100 ppm. c) Gas-sensing selectivity of the PANI/FMWCNT nanocomposite, the particle-like PANI aggregate, and the FMWCNT film devices to various volatile gases. d) Chemical gas-sensing performance of the PANI/FMWCNT nanocomposite network film under 5 ppm NH_3 after different bending cycles.

cating that the nanocomposite network also improves the transparency.

To confirm the formation of the PANI/FMWCNT nanocomposites, the films were characterized using FTIR and Raman. The FTIR spectra are presented in Figure S4 (Supporting Information). For the FMWCNTs, the peaks at 3412 cm^{-1}, 1720 cm^{-1}, and 1627 cm^{-1} can be attributed to the stretching vibrations of the O—H group, the C=O group in the carboxyl, and the stretching of the C=C in the quinoid ring, respectively. For PANI and the PANI/FMWCNTs nanocomposite, the main peaks centered at 1562 cm^{-1} and 1490 cm^{-1} can respectively be attributed to the C=C stretching vibration of the quinoid ring and the benzenoid ring in the PANI chains, indicating the presence of the emeraldine salt state of PANI.[47] As demonstrated in the Raman spectra of the samples (Figure S5, Supporting Information), FMWCNT has two characteristic peaks at 1592 cm^{-1} (G band) and 1354 cm^{-1} (D band).[48] The peaks for the PANI/FMWCNT nanocomposite at 1176 cm^{-1}, 1338 cm^{-1}, and 1592 cm^{-1} can be assigned to the C—H bending of the quinoid/benzenoid ring, the C—$N^{\cdot+}$ stretching, and the C=C stretching of the benzenoid ring, respectively, indicating the presence of both PANI and FMWCNTs in the nanocomposite.[49]

In order to test and compare the gas sensitivity of the prepared material, the PANI/FMWCNT nanocomposite network, the particle-like PANI aggregate, and the FMWCNT film were used to detect ammonia gas (NH_3). Ammonia is an important product in the synthesis of fertilizers and its requirement per year can be millions of tons. However, NH_3 is a volatile, corrosive, and poisonous gas, which can cause severe bodily harm and even death in high doses.[29] Thus, a reliable, portable, and highly sensitive sensor is needed for NH_3 detection, in case it leaks out from the reaction equipment or container, as part of environmental and workplace hazard monitoring equipment, and also homeland security. There are several reports on NH_3 sensing based on CNT/PANI, CNT/nanoparticles, or PANI nanostructures.[16,41–46] Among them, Lee et al. reported on transparent and flexible CNT films decorated with Au nanoparticles (some conductance decrease was found after 200 bending cycles) that were employed to detect NH_3. These films demonstrated a lower sensitivity (ca. 0.2% for 20 ppm NH_3), poor response (ca. 2 min), and recovery (5 min) performance, however.[42]

NH_3 has been widely investigated as a strong electron-donating chemical for PANI gas detection because on exposure to NH_3 atmosphere the emeraldine salt form of PANI transforms into its emeraldine base form, resulting in a dramatic decrease in conductance.[50,51] **Figure 6**a displays the resistance sensitivity for the PANI/FMWCNT nanocomposite network, the particle-like PANI aggregate, and the FMWCNT film devices with different polymerization times, upon exposure to 100 ppm NH_3 at room temperature. It can be seen that the PANI/FMWCNT nanocomposite network film devices have a higher gas sensitivity than the particle-like PANI aggregates and the FMWCNT film devices. Additionally, the highest gas sensitivity was obtained

for the hierarchically nanostructured nanocomposite network film devices after 8 h of polymerization, compared to the films polymerized for 6 h, 10 h, and 12 h. As shown in Figure 2b, the 8 h sample has a better network structure with sufficiently exposed active surfaces, which enables increased interactions between the analytes and the sensing materials and facilitates fast and reversible adsorption kinetics for the analytes with improved recovery and response times.[52] For the 6 h sample, the lower performance was related to the lower amount of sensing material, lower surface area as there are fewer particle-like aggregates, and less interconnected network structures. For the 10 h and 12 h sample, excessive nanocomposites were formed, which covered the original random network structure to form dense nanocomposite films, leading to a decrease in the exposed active surfaces and exposed sensing materials, and invalid network structure for sensor facilitation as the inner nanocomposites were blocked from interacting with the target gas analytes.[39,53,54] This indicates that nanocomposite films with the appropriate network structure could be assembled for high-performance portable gas sensing. Therefore, the PANI/FMWCNT nanocomposite network film prepared at 8 h polymerization, which showed the highest gas sensitivity and better transparency, was selected here as the best candidate for fabricating a high-performance gas sensor. Figure 6b demonstrates the real-time difference in resistance sensitivity of the FMWCNT, the PANI/FMWCNT nanocomposite network, and the particle-like PANI aggregate film devices with polymerization times of 8 h, upon exposure to different concentrations of NH_3 from 1 to 100 ppm at room temperature. The increase in sensitivity with increasing NH_3 concentration was higher for the PANI/FMWCNT as compared to the particle-like PANI aggregate and the FMWCNT film devices, indicating the synergistic effect of the properties of the individual materials leading to better gas sensing. Moreover, even at NH_3 concentrations as low as 1 ppm a resistance change could still be observed in the composite network film device, evidencing its superior gas-sensing performance for chemical detection and recognition. Moreover, the specificity of the hierarchically nanostructured PANI/FMWCNT nanocomposite network film sensor towards NH_3 in comparison with the sensitivity for other volatile organic compounds is displayed in Figure 6c. It can be seen that the sensitivity of the PANI/FMWCNT nanocomposite network film for 100 ppm NH_3 was 119 times higher than that for ethanol, 182 times higher than that for methanol, 235 times higher than that for acetone, and 142 times higher than that for n-propanol, indicating the capability for accurate detection of the desired gas in addition to the higher sensitivity (Figure 6c). The remarkable performance of the PANI/FMWCNT nanocomposite may probably be attributed to the sensing selectivity of the quasi-one-dimensional confined network structure film, the specific acid-base reaction, and the large surface-to-volume ratio of the nanocomposite network, which all enhance the sensitivity by enabling increased interactions between analytes and sensing material and facilitate fast and reversible adsorption kinetics for analytes with improved recovery and response times compared to their bulk counterparts.[49] To investigate the flexibility of the transparent chemical gas-sensor device, the chemical gas-sensing performances in the bent and extended states were measured. As shown in Figure 6d, the chemical gas-sensing performance did not exhibit any obvious changes after 500 bending/extending cycles at room temperature, revealing the reliability and excellent flexibility of this device.[6,55]

3. Conclusion

A conducting film based on a hierarchically nanostructured PANI-coated CNT network was successfully prepared by in situ polymerization of aniline in CNT suspension with the assistance of CNT templates and by simultaneously depositing the network on a flexible PET substrate. The as-prepared PANI/FMWCNT nanocomposite network film was assembled into a sensor device that displayed an impressive transparency (around 85.0% at 550 nm) along with an adequate flexibility (no significant reduction in performance even after 500 bending/extending cycles) for highly selective and specific, portable gas sensing at room temperature. The good sensing performance, transparency, and flexibility can be attributed to the synergistic properties of CNT and PANI, the quasi-one-dimensional nanostructure of the network, which serves as reliable and efficient sensing channels, and also to the high surface-to-volume ratio of the composite. It is anticipated that this line of research can be extended to other conducting polymer-containing nanocomposites, creating opportunities for developing low-cost, sensitive, and reliable sensors that may be incorporated into handheld, wearable, and transparent electronic devices.

4. Experimental Section

Materials: Multi-walled carbon nanotubes (MWCNTs) were commercially obtained from Cnano (FloTubeTM 9000). Aniline (distilled before use) was obtained from J&K Chemical. Ammonium persulfate (APS), concentrated hydrochloric acid, concentrated sulfuric acid, and concentrated nitric acid were purchased from Beijing Chemical Reagent Factory and were used without further purification. Polyethylene terephthalate (PET, 125 μm) films were purchased from Hui Zhixing Company (Hangzhou, China).

Preparation of FMWCNTs: 15 mg of MWCNTs was added to a mixture of 9 mL HNO_3 and 27 mL H_2SO_4, and sonicated at 60 °C for 6 h.[35] Then the dispersion of MWCNTs was filtered through a Millipore film and washed with deionized water until a neutral pH was obtained. The MWCNTs were then dried at 60 °C for 24 h and redispersed into water to prepare a 0.2 mg mL^{-1} solution. Approximately 1 wt% of sodium dodecyl benzene sulfonate (SDBS) was added to the FMWCNTs solution to enhance the dispersion of the FMWCNTs.[34]

Preparation of PANI/FMWCNT Nanocomposite Films: The PET substrate was firstly treated with oxygen plasma to make it more hydrophilic. 300 μL of the FMWCNT dispersion was added to 40 mL of 1 M HCl, and then 60 mg of APS was added. The mixture was sonicated for 5 min, and then was precooled in a refrigerator at 5 °C for 20 min. Then, 43 μL of aniline was dropped into the above solution and hydrophilic PET was dipped into the solution to react for 6 h, 8 h, 10 h, or 12 h. The films were then washed

with ethanol and dried at room temperature for further characterization. The PANI films were prepared by the same methods but in the absence of the FMWCNT dispersion. The FMWCNT films were prepared by dropping 400 μL of the FMWCNT dispersion onto the PET substrate (2 cm × 4 cm).

Gas-Sensing Measurements: The gas-sensing measurements were carried out using a WS-30A measuring system (Zhengzhou Winsen Electronics Technology, P.R. China), which can provide multi-group measurements and real-time data, according to a previous report.[52] The defined concentrations of NH_3 of 1, 5, 10, 50, or 100 ppm, were generated by dropping the corresponding amount of ammonium hydroxide (weight percent of ammonia was 25%) onto a hot plate in the chamber. The sensitivity of the conducting films to ethanol, methanol, acetone, and isopropanol was also tested by the same method to obtain the gas-sensing selectivity data. The sensitivity S was defined as the normalized resistance change

$$S = (R_g - R_0)/R_0 = \Delta R/R_0 \quad (1)$$

where R_g is the resistance of the conductive film after exposure to gas analytes and R_0 is the resistance in air.

General Techniques: SEM images were obtained using a Zeiss Supra 55 instrument at a voltage of 20 kV. Fourier-transform infrared (FTIR) spectra were collected on a Nicolet 6700 FTIR spectrometer. Raman spectra were collected on a Jobin Yvon Lab RAM HR Raman microscope using an excitation wavelength of 532 nm at a spot with a diameter of 1 μm. The sheet resistance of the films was measured using a four-probe tester (RST-8).

Supporting Information

Supporting Information is available from the Wiley Online Library or from the author.

Acknowledgements

This work was financially supported by the National Natural Science Foundation of China, the Beijing Natural Science Foundation (2152023), the 973 Program (2011CBA00503 and 2011CB932403), and the Fundamental Research Funds for the Central Universities.

[1] D. J. Lipomi, M. Vosgueritchian, B. C. Tee, S. L. Hellstrom, J. A. Lee, C. H. Fox, Z. Bao, *Nat. Nanotechnol.* **2011**, *6*, 788.
[2] S. Bae, H. Kim, Y. Lee, X. Xu, J.-S. Park, Y. Zheng, J. Balakrishnan, T. Lei, H. R. Kim, Y. I. Song, *Nat. Nanotechnol.* **2010**, *5*, 574.
[3] Z. Liu, J. Xu, D. Chen, G. Shen, *Chem. Soc. Rev.* **2015**, *44*, 161.
[4] J. W. Liu, J. L. Wang, Z. H. Wang, W. R. Huang, S. H. Yu, *Angew. Chem. Int. Ed.* **2014**, *126*, 13695.
[5] W. Zeng, L. Shu, Q. Li, S. Chen, F. Wang, X. M. Tao, *Adv. Mater.* **2014**, *26*, 5310.
[6] Z. Yu, Q. Zhang, L. Li, Q. Chen, X. Niu, J. Liu, Q. Pei, *Adv. Mater.* **2011**, *23*, 664.
[7] W. J. Yu, S. H. Chae, S. Y. Lee, D. L. Duong, Y. H. Lee, *Adv. Mater.* **2011**, *23*, 1889.
[8] X. Wang, X. Lu, B. Liu, D. Chen, Y. Tong, G. Shen, *Adv. Mater.* **2014**, *26*, 4763.
[9] X. Wang, Y. Gu, Z. Xiong, Z. Cui, T. Zhang, *Adv. Mater.* **2014**, *26*, 1336.
[10] J. W. Suk, K. Kirk, Y. Hao, N. A. Hall, R. S. Ruoff, *Adv. Mater.* **2012**, *24*, 6342.
[11] A. R. Rathmell, B. J. Wiley, *Adv. Mater.* **2011**, *23*, 4798.
[12] S. Pang, Y. Hernandez, X. Feng, K. Müllen, *Adv. Mater.* **2011**, *23*, 2779.
[13] L. Nyholm, G. Nyström, A. Mihranyan, M. Strømme, *Adv. Mater.* **2011**, *23*, 3751.
[14] Y. Meng, K. Wang, Y. Zhang, Z. Wei, *Adv. Mater.* **2013**, *25*, 6985.
[15] D. S. Hecht, L. Hu, G. Irvin, *Adv. Mater.* **2011**, *23*, 1482.
[16] a) S. Pandey, G. K. Goswami, K. K. Nanda, *Sci. Rep.* **2013**, *3*, 2082; b) Y. Zhang, J. J. Kim, D. Chen, H. L. Tuller, G. C. Rutledge, *Adv. Funct. Mater.* **2014**, *24*, 4005.
[17] K. Ariga, Y. Yamauchi, G. Rydzek, Q. Ji, Y. Yonamine, K. C.-W. Wu, J. P. Hill, *Chem. Lett.* **2014**, *43*, 36.
[18] J. Wang, M. Liang, Y. Fang, T. Qiu, J. Zhang, L. Zhi, *Adv. Mater.* **2012**, *24*, 2874.
[19] R. V. Salvatierra, C. E. Cava, L. S. Roman, A. J. Zarbin, *Adv. Funct. Mater.* **2013**, *23*, 1490.
[20] C. Liao, M. Zhang, M. Y. Yao, T. Hua, L. Li, F. Yan, *Adv. Mater.* **2015**, DOI: 10.1002/adma.201402625.
[21] Y. Li, S. Chen, M. Wu, J. Sun, *Adv. Mater.* **2012**, *24*, 4578.
[22] Y. Yang, S. Jeong, L. Hu, H. Wu, S. W. Lee, Y. Cui, *Proc. Natl. Acad. Sci.* **2011**, *108*, 13013.
[23] H. Wu, D. Kong, Z. Ruan, P.-C. Hsu, S. Wang, Z. Yu, T. J. Carney, L. Hu, S. Fan, Y. Cui, *Nat. Nanotechnol.* **2013**, *8*, 421.
[24] Z. Wu, X. Chen, S. Zhu, Z. Zhou, Y. Yao, W. Quan, B. Liu, *Sens. Actuators B* **2013**, *178*, 485.
[25] S. Bai, K. Zhang, J. Sun, D. Zhang, R. Luo, D. Li, C. Liu, *Sens. Actuators B* **2014**, *197*, 142.
[26] F. Yang, X. Wang, D. Zhang, J. Yang, D. Luo, Z. Xu, J. Wei, J.-Q. Wang, Z. Xu, F. Peng, Y. Li, *Nature* **2014**, *510*, 522.
[27] Z. Niu, P. Luan, Q. Shao, H. Dong, J. Li, J. Chen, D. Zhao, L. Cai, W. Zhou, X. Chen, *Energy Environ. Sci.* **2012**, *5*, 8726.
[28] K. Jiang, J. Wang, Q. Li, L. Liu, C. Liu, S. Fan, *Adv. Mater.* **2011**, *23*, 1154.
[29] D. R. Kauffman, A. Star, *Angew. Chem. Int. Ed.* **2008**, *47*, 6553.
[30] Y. H. Yoon, J. W. Song, D. Kim, J. Kim, J. K. Park, S. K. Oh, C. S. Han, *Adv. Mater.* **2007**, *19*, 4284.
[31] C. J. Shearer, A. Cherevan, D. Eder, *Adv. Mater.* **2014**, *26*, 2295.
[32] J. Ren, L. Li, C. Chen, X. Chen, Z. Cai, L. Qiu, Y. Wang, X. Zhu, H. Peng, *Adv. Mater.* **2013**, *25*, 1155.
[33] D. Janas, K. Koziol, *Nanoscale* **2014**, *6*, 3037.
[34] B. Dan, G. C. Irvin, M. Pasquali, *ACS Nano* **2009**, *3*, 835.
[35] J. Wang, X. Zhang, X. Huang, S. Wang, Q. Qian, W. Du, Y. Wang, *Small* **2013**, *9*, 3759.
[36] N.-R. Chiou, C. Lu, J. Guan, L. J. Lee, A. J. Epstein, *Nat. Nanotechnol.* **2007**, *2*, 354.
[37] J. Huang, S. Virji, B. H. Weiller, R. B. Kaner, *J. Am. Chem. Soc.* **2003**, *125*, 314.
[38] J. Xu, K. Wang, S.-Z. Zu, B.-H. Han, Z. Wei, *ACS Nano* **2010**, *4*, 5019.
[39] M. A. Invernale, Y. Ding, D. M. D. Mamangun, M. S. Yavuz, G. A. Sotzing, *Adv. Mater.* **2010**, *22*, 1379.
[40] K. Wang, Q. Meng, Y. Zhang, Z. Wei, M. Miao, *Adv. Mater.* **2013**, *25*, 1494.
[41] T. Zhang, M. B. Nix, B. Y. Yoo, M. A. Deshusses, N. V. Myung, *Electroanalysis* **2006**, *18*, 1153.
[42] K. Lee, V. Scardaci, H.-Y. Kim, T. Hallam, H. Nolan, B. E. Bolf, G. S. Maltbie, J. E. Abbott, G. S. Duesberg, *Sens. Actuators B* **2013**, *188*, 571.
[43] C. Oueiny, S. Berlioz, F.-X. Perrin, *Prog. Polym. Sci.* **2014**, *39*, 707.

[44] M. Ding, Y. Tang, P. Gou, M. J. Reber, A. Star, *Adv. Mater.* **2011**, *23*, 536.
[45] M. Kaempgen, S. Roth, *J. Electroanal. Chem.* **2006**, *586*, 72.
[46] L. He, Y. Jia, F. Meng, M. Li, J. Liu, *Mater. Sci. Eng. B* **2009**, *163*, 76.
[47] H. Fan, H. Wang, N. Zhao, X. Zhang, J. Xu, *J. Mater. Chem.* **2012**, *22*, 2774.
[48] Z. Wei, M. Wan, T. Lin, L. Dai, *Adv. Mater.* **2003**, *15*, 136.
[49] M. Cochet, W. K. Maser, A. M. Benito, M. A. Callejas, M. T. Martínez, J.-M. Benoit, J. Schreiber, O. Chauvet, *Chem. Commun.* **2001**, 1450.
[50] S. Virji, J. Huang, R. B. Kaner, B. H. Weiller, *Nano Lett.* **2004**, *4*, 491.
[51] W. Yuan, A. Liu, L. Huang, C. Li, G. Shi, *Adv. Mater.* **2013**, *25*, 766.
[52] S. Bai, C. Sun, P. Wan, C. Wang, R. Luo, Y. Li, J. Liu, X. Sun, *Small* **2015**, *11*, 310.
[53] J. Kong, N. R. Franklin, C. Zhou, M. G. Chapline, S. Peng, K. Cho, H. Dai, *Science* **2000**, *287*, 622.
[54] V. Scardaci, R. Coull, J. N. Coleman, *Appl. Phys. Lett.* **2010**, *97*, 023114.
[55] L. Li, Z. Yu, W. Hu, C. Chang, Q. Chen, Q. Pei, *Adv. Mater.* **2011**, *23*, 5563.

Received: June 20, 2015
Revised: June 30, 2015
Published online: August 21, 2015

